



An E7-retinoblastoma protein pathway mechanism may account for the higher carcinogenic ability of HPV16 over HPV58 in cervical cancer

Jian Zou^{1^}, Yang Li^{1,2^}, Tingting Chen^{1^}, Changkun Zhu^{1^}

¹Department of Gynecologic Oncology, Women's Hospital, Zhejiang University School of Medicine, Hangzhou, China; ²Department of Zhejiang Provincial Key Laboratory of Precision Diagnosis and Therapy for Major Gynecological Diseases, Women's Hospital, Zhejiang University School of Medicine, Hangzhou, China

Contributions: (I) Conception and design: J Zou, Y Li; (II) Administrative support: J Zou, C Zhu; (III) Provision of study materials or patients: T Chen; (IV) Collection and assembly of data: J Zou, T Chen; (V) Data analysis and interpretation: J Zou, C Zhu; (VI) Manuscript writing: All authors; (VII) Final approval of manuscript: All authors.

Correspondence to: Changkun Zhu, MD. Department of Gynecology and Oncology, Women's Hospital, Zhejiang University School of Medicine, No. 1 Xueshi Road, Hangzhou 310016, China. Email: zhuchangkun@zju.edu.cn.

Background: Among human papillomavirus (HPV) type, HPV16 displays the strongest carcinogenic capacity for cervical cancer, but the mechanism underlying this phenomenon remains unclear.

Methods: We collected 4,030 cervical exfoliated cell samples for genotyping HPV using HybriBio's proprietary flow-through hybridization technique, liquid-based cytology (LBC), colposcopy, and biopsies if indicated. Four plasmids containing E6 and E7 of HPV16 and 58 were constructed and transfected into 293T and U2OS cells. We detected the cell phenotype using Cell Counting Kit 8 (CCK8) assay, Transwell assay, flow cytometry, and apoptosis assay; the expression of retinoblastoma protein (Rb) and phosphorylated Rb (pRb) was determined via Western blot; and the cell activity was determined via a zebrafish model treated with or without roscovitine.

Results: The positive rates of HPV16 and 58 were, respectively, 18.9% and 19.7% in the ≤ low-grade squamous intraepithelial lesion (LSIL) group, 49.5% and 19.6% ($P < 0.001$) in the high-grade squamous intraepithelial lesion (HSIL) group, 65.3% and 9.0% ($P < 0.001$) in the cancer group. *In vitro*, both 293T and U2OS cells with overexpressed HPV16 E6 and E7 displayed significantly higher cell proliferation, faster cell invasion, decreased cell apoptosis, and accelerated cell cycle from G1 phase to S phase compared to those with overexpressed HPV58 E6 and E7 (all P values < 0.05). Rb loss of function was observed in cells with HPV16 E7 overexpression, while a greater level of phosphorylated Rb was observed in cells with HPV58 E7 overexpression. Roscovitine restored Rb expression and decreased the cell activity in zebrafish.

Conclusions: HPV16 possesses a stronger carcinogenic ability than does HPV 58, and the mechanism underlying this effect may be the impairment of the E7-Rb pathway.

Keywords: E7-Rb; HPV16; HPV58; cervical cancer

Submitted Aug 01, 2023. Accepted for publication Jan 16, 2024. Published online Apr 25, 2024.

doi: 10.21037/tcr-23-1211

View this article at: <https://dx.doi.org/10.21037/tcr-23-1211>

[^] ORCID: Jian Zou, 0000-0002-0470-2574; Yang Li, 0000-0002-0112-1328; Tingting Chen, 0000-0003-0233-9369; Changkun Zhu, 0000-0003-2853-3741.

Introduction

Cervical cancer is the fourth most common cancer in women globally, with an estimated 604,127 new cases and 341,831 deaths worldwide in 2020 (1). The high-risk human papillomavirus (HPV) infection is a causal factor for cervical cancer (2). HPV16 and HPV18 are known to be the two most carcinogenic HPV types and are responsible for 70% of cervical cancer cases (3). Meanwhile, carcinogenesis associated with HPV58 is less common, contributing to only 3.3% of global cases (4); however, it is relatively prevalent in Asian women, ranking as the third most common type of cervical cancer (5-7). Epidemiologic data attests to a diverse distribution between HPV16 and HPV58 in different cervical lesions. A meta-analysis of 30,165 HPV-positive women showed that HPV16 positivity rates varied remarkably between low-grade and high-grade lesions, with 22.7% for normal tissues and cervicitis, 23.6% for cervical intraepithelial neoplasia grade 1 (CIN1), 37.6% for CIN2, 51.9% for CIN3, and 65.6% for invasive cervical carcinoma (ICC); however, HPV58 positivity rates vary little between low-grade and high-grade lesions, with 14.6% for normal tissues and cervicitis, 16.0% for CIN1, 19.9% for CIN2, 20.2% for CIN3, and 13.5% for ICC (8). The diversity of distribution between HPV16 and HPV58 in different pathology statuses implies a difference in carcinogenic ability between the two subtypes, but the mechanism underlying this remains unclear.

The HPV oncogene E6 and E7 possess transforming properties which can target P53 and Rb, respectively (9,10). E6 oncoprotein degrades P53 and the E6-E6AP-p53

complex represents a prototype of viral hijacking of both the ubiquitin-mediated protein degradation pathway and the p53 tumor-suppressor pathway (11). E7 binds to hypophosphorylated retinoblastoma protein (Rb) and induces cell cycle progression by disrupting Rb-E2F complexes (12,13). Rb contains three isoforms: unphosphorylated Rb, hypophosphorylated Rb, and hyperphosphorylated Rb. The hyperphosphorylated Rb is an inactive form which is generated by the cyclin-dependent kinase 2 (CDK2) complex in the late G1 phase. Roscovitine, a CDK2 inhibitor, decreases the level hyperphosphorylated Rb (inactive isoform) while increasing that of monophosphorylated Rb (the activated Rb isoform and is regarded as a candidate for restoring Rb function).

In this present study, we collected cervical exfoliated cell samples and analyzed the proportion of HPV16 and HPV58 positivity in different degrees of pathology. Furthermore, we constructed four plasmids containing E6 and E7 of HPV16 and HPV58 into pFLAG-CMV-5.1 expression vector, transfected them into 293T cells and U2OS cells, and observed the cell phenotypes and the expression of Rb and phosphorylated Rb (pRb). We subsequently injected these cells into the abdominal cavity of zebrafish to observe the activity of cells with or without roscovitine treatment. The study aimed to clarify the mechanism through which HPV16 exerts a higher carcinogenic ability compared to HPV58 and to identify a means to blocking E7-Rb in HPV. We present this article in accordance with the ARRIVE reporting checklist (available at <https://tcr.amegroups.com/article/view/10.21037/tcr-23-1211/rc>).

Methods

Clinical sample collection

We collected 4,030 cervical exfoliated cell samples from patients aged 25–65 years at Women's Hospital, Zhejiang University School of Medicine between 2012 and 2018; the exclusion criteria for sample collection was as follows: (I) previous therapeutic procedure of the cervix, such as conization and physical therapy; (II) infection of other pathogens, such as HIV, syphilis, and *Candida*; (III) pregnancy; (IV) presence of other malignant tumors; and (V) immune disease. Each woman received HPV testing using HybriBio's hybridization technique (HybriBio Rapid GenoArray Test Kit), liquid-based cytology (LBC), colposcopy, and biopsy if necessary. The HybriBio Rapid GenoAssay Kit can detect 21 types HPV, including the

Highlight box

Key findings

- Retinoblastoma protein (Rb) loss of function was observed in cells with human papilloma virus (HPV)16 E7 overexpression while a greater level of phosphorylated Rb was observed in cells with HPV58 E7 overexpression.

What is known and what is new?

- HPV16 is more carcinogenic than is HPV58 both *in vitro* and *in vivo*.
- Our study discovered a difference in E7-Rb loss of function between HPV16 and HPV58. Roscovitine can restore the function of Rb to block HPV carcinogenesis.

What is the implication, and what should change now?

- Roscovitine may be a candidate drug for blocking HPV via the restoration of Rb expression.

high-risk types (HPV16, 18, 31, 33, 35, 39, 45, 51, 52, 56, 58, 59, 68) and low-risk types (HPV6, 11, 42, 43, 44, 53, 66 and CP8304). Histological diagnoses were categorized as the follows: normal, cervical intraepithelial neoplasia grade 1 (CIN1), CIN2, CIN3, squamous cell carcinoma (SCC), or adenocarcinoma (ADC). The patients were classified into a \leq low-grade squamous intraepithelial lesion (LSIL) group (normal and CIN1), a high-grade squamous intraepithelial lesion (HSIL) group (CIN2 and CIN3), and a cancer group according to the histopathologic diagnosis. The study was conducted in accordance with the Declaration of Helsinki (as revised in 2013) and was approved by the institutional review board of the Women's Hospital of Zhejiang University (approval No. IRB-20230341-R). The requirement for individual consent was waived due to the retrospective nature of the analysis. All animal experiments were performed under a project license (No. ZJU20230472) granted by committee ethics board of Zhejiang University and in compliance with the institutional guidelines for the care and use of animals.

Cell culture

We used the U2OS (human osteosarcoma cell) and 293T (human embryonic kidney cell, with wild-type *P53*) cell lines (American Type Culture Collection) that did not have HPV E6 or E7 and could be passed down for cultivation *in vitro* and a zebrafish model. The U2OS and 293T cells were cultured in high-glucose Dulbecco's modified Eagle's medium (DMEM) with 10% fetal bovine serum at 37 °C in a 5% CO₂ atmosphere.

Reagents and antibodies

The HPV16 (gene bank: K02718.1) E6 and E7 and HPV58 (gene bank: D90400.1) E6 and E7 genes were synthesized and constructed into a Pflag-CMV-5.1 expression vector (E6908; Sigma-Aldrich). DNA X-tremeGENE HP DNA Transfection Reagent (Roche) was mixed with 2 μ g of plasmid (ratio 3:1) according to the manufacturer's guidelines. The experiment included negative control (NC; pFLAG-CMV-5.1 expression vector + X-tremeGENE HP DNA Transfection Reagent), HPV58E6, HPV16E6, HPV58E7, and HPV16E7 groups. Polymerase chain reaction (PCR) was performed using the HPV16 and HPV58 E6 and E7 primers. The antibodies included were anti-Rb (ab181616; Abcam), anti-pRb (E231-ab32015; Abcam), anti-GAPDH (sc-32233; Santa Cruz

Biotechnology), anti-FLAG (SAB4200071; Sigma-Aldrich), anti-rabbit horseradish peroxidase (HRP) (#7074; Cell Signaling Technology), and anti-mouse HRP (#7076; Cell Signaling Technology). Roscovitine (Seliciclib, CYC202) was purchased from Selleck Chemicals.

Transfection and reverse-transcription PCR

We cultured 5×10^4 U2OS and 293T cells into six-well plates, mixed 2 μ g of constructed plasmids with DNA X-tremeGENE HP DNA Transfection Reagent (Roche; ratio of 1:3), and then added this mixture to the U2OS and 293T cells. After overnight incubation, the culture medium was replaced with fresh DMEM containing 10% FBS before further study. After 48-hour transfection, we extracted the total RNA by using TRizol Reagent (Invitrogen, Thermo Fisher Scientific) and synthesized the complement DNA (cDNA) by using a PrimeScript RT reagent kit (#RR047; Takara Bio). We performed reverse-transcription PCR (RT-PCR) with the appropriate primers for GAPDH (forward: 5'-TCACCACCATGGAGAAGGC-3'; 5'-GCTAAGCAGTTGGTGGTGC-3'), HPV58E6 (forward: 5'-ACGCAGAGGAGAAACCAC-3'; reverse: 5'-CTGTCCAACGACCCGAAA-3'), HPV58E7 (forward: 5'-GGATGAAATAGGCTTGGA-3'; reverse: 5'-GTCGGTTGTTGTACTGTTGA-3'), HPV16E6 (forward: 5'-CTGCAAGCAACAGTTACTGC-3'; reverse: 5'-GGCTTTTGACAGTTAATACACC-3'), and HPV16E7 (forward: 5'-CATGGAGATACACCTA CATTGC-3'; reverse: 5'-CACAACCGAAGCGTAG AGTC-3').

Western blot analysis

We cultured the 5×10^4 U2OS and 293T cells into six-well plates, mixed 2 μ g of constructed plasmids with X-tremeGENE HP DNA Transfection Reagent (Roche; ratio of 1:3), and then added this mixture to the U2OS and 293T cells. After overnight incubation, the culture medium was replaced with fresh DMEM containing 10% FBS before further study. We then treated the cells with 0 μ M, 5 μ M, 10 μ M, 15 μ M, or 30 μ M of roscovitine (CYC202). After 48-hour transfection, we extracted cell protein. The appropriate amounts of proteins were applied and subjected to sodium dodecyl sulfate-polyacrylamide gel electrophoresis (SDS-PAGE) and, protein lysates were separated in 10% SDS-PAGE gel, which was followed by subsequently transfer to 0.22 μ m of polyvinylidene difluoride membrane (PVDF)

(ISEQ00010; Sigma-Aldrich). After incubating the PVDF membrane with the primary antibodies and secondary antibodies at 4 °C overnight, we detected the complex using an ImageQuant LAS 4000 mini (GE HealthCare) and an EZ-ECL Kit (20-500-120; Biological Industries), and the expression of Rb and pRb was evaluated with Quantity One software (Bio-Rad Laboratories).

Cell proliferation assay

The 293T and U2OS cells were plated on 96-well plates at 2,000–3,000 cells per well. Cell Counting Kit 8 (CCK8) assay was performed at 0 h, 24 h, 48 h, 72 h, and 96 h after transfection with these plasmids. The absorbance was detected at 450 nm with a spectrophotometer, and the experiment was completed three times.

Cell cycle analysis

At 48 h posttransfection, the cells were fixed in 75% precooled ethanol for 1–2 h at 4 °C. After washing, the cell pellet was resuspended in propidium iodide (PI) staining buffer (50 µg/mL of PI and 10 µg/mL of RNase A), incubated for 15 min at 37 °C, and detected via a flow cytometer (Beckman Coulter).

Cell apoptosis assay

At 48 h posttransfection, an annexin V-fluorescein isothiocyanate and PI apoptosis detection kit (Bionique) was used to test the percentage of early cell apoptosis, with the test being repeated three times.

Cell invasion assay

A cell invasion assay was performed using modified Boyden chambers (Transwell; Corning Incorporated) with 8-µm pores in 24-well plates. At 48 h after transfection, the Transwell filters in the upper compartment were coated with Matrigel. After 30 min of incubation at 37 °C, the Matrigel solidified and served as the extracellular matrix for tumor cell invasion analysis. Cells (2×10^5) in 200 µL of serum-free medium were added into the upper chamber. A total of 500 µL of complete medium was then added in the bottom compartment of the chamber. After 12–24 h of culture, the cells penetrating the Matrigel to the bottom of

the chamber were fixed with 100% methanol and stained with 0.5% gentian violet crystal solution for 20 min. The number of cells passing through the Matrigel was counted in five randomly selected visual fields three times.

Zebrafish model

After being transfected for 48 h with the plasmids of the HPV16 and HPV58 E7 genes, U2OS and 293T cells (2×10^6 cells) labeled with Dil (Solarbio, D8700) were injected into the intestine region of AB strain zebrafish with a specialized long needle 48 postfertilization. The water provided the zebrafish was treated with dimethyl sulfoxide (DMSO; the solvent of roscovitine) or 30 µM of roscovitine for 24 h, with each treatment group containing 20 zebrafish. The fluorescence intensity of cells in the abdomen of zebrafish was detected using a fluorescence microscope. The fluorescence intensity of cells was measured using ImageJ software (US National Institutes of Health).

Statistical analysis

SPSS version 22.0 (IBM Corp.,) was used to analyze the portion of HPV16 and HPV58 in different degrees of pathology via the chi-squared test, and the differences in cell phenotype and protein expression between two groups were determined via the Student *t*-test. $P < 0.05$ was considered to indicate statistical significance.

Results

Distribution of HPV16 and HPV58 among different pathological statuses of the cervix

Genotyping detection for HPV16 and 58 was performed in 4030 cervical samples. The three most common HPV types were HPV16, HPV52 and HPV58 in the ≤LSIL group; HPV16, HPV58, and HPV52 in the HSIL group; and HPV16, HPV18, and HPV58 in the cancer group. Moreover, HPV16 was more frequent in high-grade lesion and cervical cancer than HPV58.

As shown in *Table 1*, the positive rate of HPV16 was significantly higher than that of HPV58 in the HSIL and cancer groups (both P values < 0.001) but not in the LSIL group. The indicated that HPV16 had a greater carcinogenic ability than did HPV58.

Table 1 The rate of HPV16 and 58 positivity according to different degrees of pathological in 4,030 cervical exfoliated cell samples

Group	HPV infection	Positive case	Percentage	P value
≤ LSIL	HPV16	467/2,469	18.9%	0.24
	HPV58	487/2,469	19.7%	
HSIL	HPV16	586/1,184	49.5%	<0.001
	HPV58	232/1,184	19.6%	
Cancer	HPV16	246/377	65.3%	<0.001
	HPV58	34/377	9.0%	

LSIL, low-grade squamous intraepithelial lesion; HSIL, high-grade squamous intraepithelial lesion; HPV, human papillomavirus.

293T and U2OS cells with HPV16 E6 and E7 overexpression exhibited greater vitality than did cells with HPV58 E6 and E7 overexpression

After we constructed the plasmids of HPV16 and HPV58 E6 and E7, we performed colony PCR to confirm the target genes (Figure S1A). We then transfected the plasmids to the 293T and U2OS cells and detected the expression of HPV16 and HPV58 E6 and E7 via RT-PCR (Figure S1B).

To compare carcinogenic ability of HPV16 E6 and E7 with that of HPV58 E6 and E7, the E6 and E7 genes of HPV16 and 58 were transiently transfected into 293T and U2OS cells. It was found that HPV16 E6 and E7 could promote the cell proliferation in 293T and U2OS cells from day 2 to 5 more rapidly than could HPV58 E6 and E7 (Figure 1A). In 293T cells, the early apoptosis rate of the HPV58E6 group was 9.7% that of the HPV16E6 group was 5.04%, that of the HPV58E7 was 6.85%, and that of the HPV16E7 group was 3.99%. HPV16 E6/E7 demonstrated a greater ability to decrease cell apoptosis than did HPV58 E6/E7 (Figure 1B). The same results were observed in the U2OS cells.

HPV16 E6 and E7 demonstrated a greater capacity to promote cell invasion than did HPV58 E6 and E7 in 293T and U2OS cells (Figure 2A). In Figure 2B, the y-axis is the proportions of the G0–G1, G2/M, and S phases. In 293T cells, the proportion of S phase in the HPV58E6 group, HPV16E6 group, HPV58E7 group, and HPV16E7 group was 42.68%, 52.66%, 47.89%, and 52.7%, respectively. HPV16 E6/E7 exhibited a greater ability to promote cell cycle progression than did HPV58 E6/E7, and these same results were observed in the U2OS cells.

The 293T and U2OS cells overexpressing HPV16 E6 and E7 displayed significantly higher cell proliferation, faster cell invasion, decreased cell apoptosis, and accelerated

cell cycle from G1 phase to S phase than did those overexpressing HPV58 E6 and E7 (all P values <0.05).

Compared to HPV58 E7, HPV16 E7 induced greater Rb loss of function and less phosphorylation

In 293T and U2OS cells, greater Rb loss of function was observed in cells overexpressing HPV16 E7, while greater phosphorylation of Rb was observed in cells overexpressing HPV58 E7 (Figure 3A). In both 293T and U2OS cells, after treatment with roscovitine (5 μM, 10 μM, 15 μM, 30 μM), the total Rb was restored in cells overexpressing HPV58 E7, especially in the 30-μM group (Figure 3B); after treatment with 30 μM of roscovitine, the Rb level was restored, especially in cells overexpressing HPV58 E7 (Figure 3C). The hyperphosphorylated Rb is an inactive form, and perhaps HPV58E7 inactivated RB via hyperphosphorylation. When the cells were treated with roscovitine, HPV58E7 led to a greater restoration of Rb (Figure 3B,3C). Roscovitine is a CDK2 inhibitor, and perhaps HPV16 E7 eliminates Rb, while HPV58 E7 hyperphosphorylates Rb.

Roscovitine decreased the activity of 293T and U2OS cells transfected with HPV16 and 58 E7 in zebrafish

Compared with the DMSO group, the roscovitine (30 μM) group showed a remarkable decrease in the activity of 293T and U2OS cells transfected with HPV16 and 58 E7 that were injected into the intestinal region of zebrafish (Figure 4A,4B) When roscovitine (30 μM) was added to the water of zebrafish, the cell activity in the intestinal region of zebrafish decreased, especially in the HPV58 group, indicating that roscovitine can decrease cell activity by restoring Rb function.

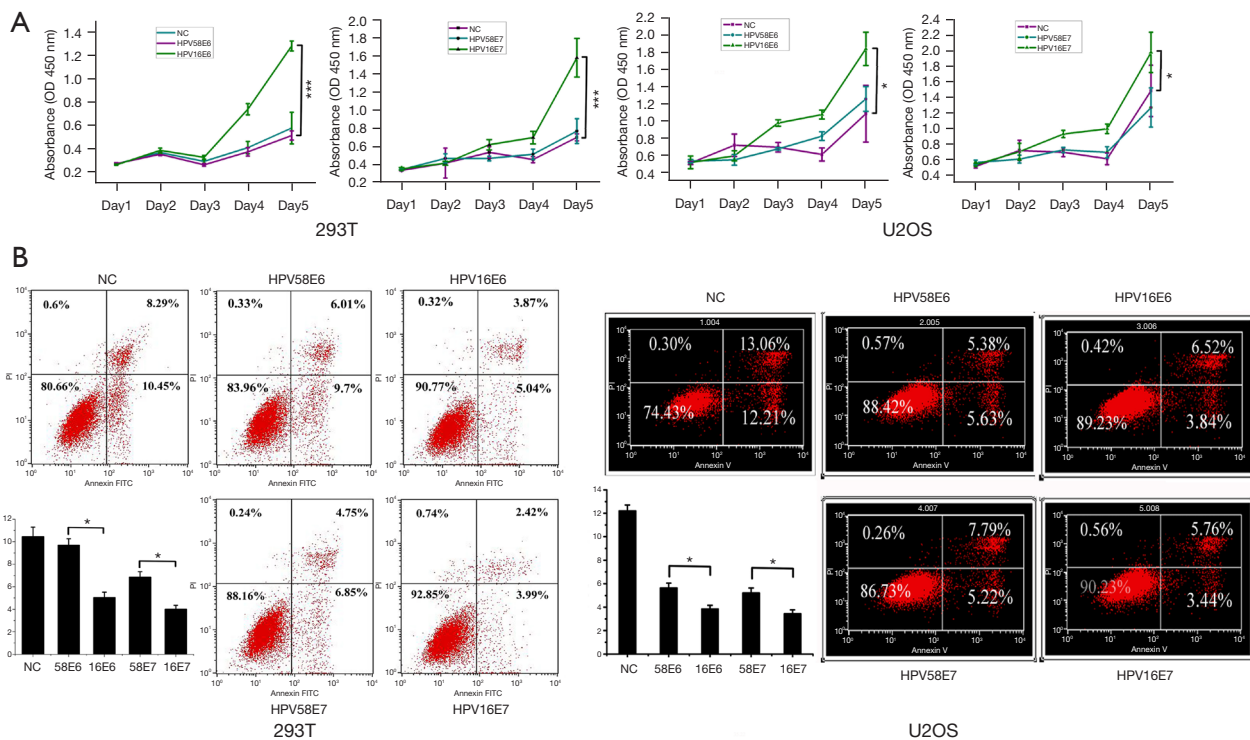


Figure 1 HPV16 E6 and E7 demonstrated a stronger ability to promote cell survival and inhibit cell apoptosis than did HPV58 E6 and E7. (A) 293T and U2OS cells were plated in each well and transfected with the HPV16 and HPV58 E6 and E7 plasmids. CCK8 assay was then performed at the time points indicated. (B) At 48 h after transfection with the HPV16 and HPV58 E6 and E7 plasmids. 293T and U2OS cells were collected for evaluation of apoptosis via flow cytometry. *, $P < 0.05$; ***, $P < 0.001$. HPV, human papillomavirus; NC, negative control; CCK8, Cell Counting Kit 8.

Discussion

Epidemiological data suggest that the rate of HPV16 positivity substantially increases with the degree of severity of cervical lesions (14-16). For instance, an investigation in 12,816 women in Southeast China found that the rate of HPV16 positivity was higher than that of HPV58 in patients with cervical intraepithelial neoplasia and invasive cervical cancer, respectively (17). A study of 1387 women with CIN2/3 from Shanxi Province, China, reported that the HPV16 positivity rate was 59.3% while that of HPV58 was only 14.4% (18). In our study, we found that in 4030 cervical samples, the three most common HPV types were HPV16, 52, and 58 in the \leq LSIL group; HPV16, 58, and 52 in the HSIL group; and HPV16, 18, and 58 in the cancer group. The positive rates of HPV16 and HPV58 were, respectively, 18.9% and 19.7% in the \leq LSIL group, 49.5% and 19.6% in the HSIL group, and 65.3% and 9.0% in the cancer group. Our and other previous studies suggest

that the association of HPV16 with high-grade lesions is closer than that of HPV58 and that HPV16 may possess a stronger carcinogenic ability than HPV58 in cervical cancer. HPV16 is the most common HPV type generally and has the strongest carcinogenic ability, but HPV58 is more common in Zhejiang Province. In our study, we focused on these two HPV types to clarify the mechanism underlying their different carcinogenic capacities.

We thus overexpressed HPV16 and 58 E6 and E7 in 293T and U2OS cells and observed the change of malignant phenotypes in both cell types. Both 293T and U2OS cells were selected as they have wild-type P53 and Rb and have not been infected by any type of HPV. We found that cells with HPV16 E6 and E7 overexpression exhibited increased cell proliferation, invasion, and cell cycle progression and more inhibited cell apoptosis than did cells with HPV58 E6 and E7 overexpression. It is widely acknowledged that both viral E6 and E7 are the

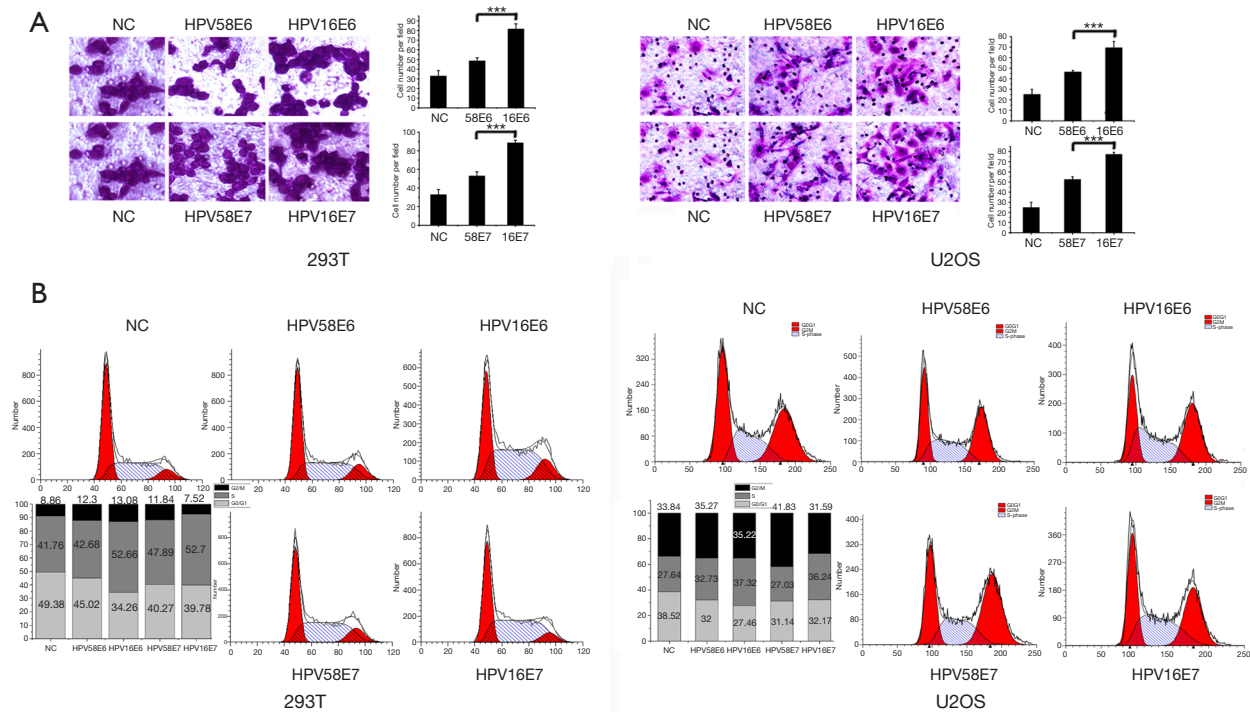


Figure 2 HPV16 E6 and E7 demonstrated a stronger ability to promote cell invasion and cell cycle progression than did HPV58 E6 and E7. (A) At 48 h after transfection with the HPV16 and HPV58 E6 and E7 plasmids. 293T and U2OS cells were collected for Matrigel invasion assays. After 12–24 h of culture, the cells penetrating the Matrigel to the bottom of the chamber were fixed with 100% methanol and stained with 0.5% gentian violet crystal solution for 20 min. Representative images are shown (magnification: 200×). The results were plotted as the average number of invasive cells from five randomly selected fields. Data are represented as the mean ± SD of three independent experiments. (B) At 48 h after transfection with the HPV16 and HPV58 E6 and E7 plasmids. 293T and U2OS cells were collected for cell cycle assay under flow cytometry. ***, P<0.001. HPV, human papillomavirus; NC, negative control.

principal viral oncoproteins responsible for the initiation and progression of cervical cancer, which act synergistically to immortalize and transform the infected cells, mainly through degrading P53 and inactivating Rb (19,20). The isoforms of HPV16 E6 (E6*I, E6*II, E6*III, E6^E7, E6^E7*I, E6^E7*II, E6*IV, E6*V and E6*VI) and HPV58 E6 (E6*I and E6*II) have been identified (21). The isoforms of P53 are Δ40p53 and Δ133p53. E6 and its E6*II isoform induces a significant decrease in p53 expression, but only E6 triggers a decrease in Δ40p53 expression; meanwhile, E6*II interacts with p53 but not with Δ40p53 or Δ133p53. On the other hand, E6*I does not exhibit any effect or interaction with the p53 isoforms (22). We found that there was no significant difference in the expression of P53 between the HPV16 E6 and HPV58 E6 overexpression group. The interaction of HPV16 and 58 E6 and P53 is complex and requires further investigation. Some research suggests that HPV E7 and Rb may be regulated by ubiquitin-dependent

proteolysis in cervical cancer (23). We found out that the total Rb expression was more decreased in the HPV16 E7 overexpression group, while pRb was more increased in the HPV58 E7 overexpression group. Hyperphosphorylated Rb is the inactive isoform. We observed that the HPV16 E7 overexpression group showed a decreased level of Rb, while the HPV58 E7 group showed a greater degree of Rb hyperphosphorylation, suggesting that impairment of the E7–Rb pathway is one of the mechanisms accounting for the greater carcinogenic ability of HPV16 as compared to that of HPV58. It is interesting to note that the FLAG band in HPV16 E7 was lower in both cell lines than in HPV58E7, with the result maintaining across multiple repetitions of experiment. This may be explained by the fact that HPV16E7 is highly susceptible to proteolysis and elimination, meanwhile HPV58E7 caused Rb to hyperphosphorylate. In subsequent studies, we can use other cell lines and plasmid vectors to confirm the results

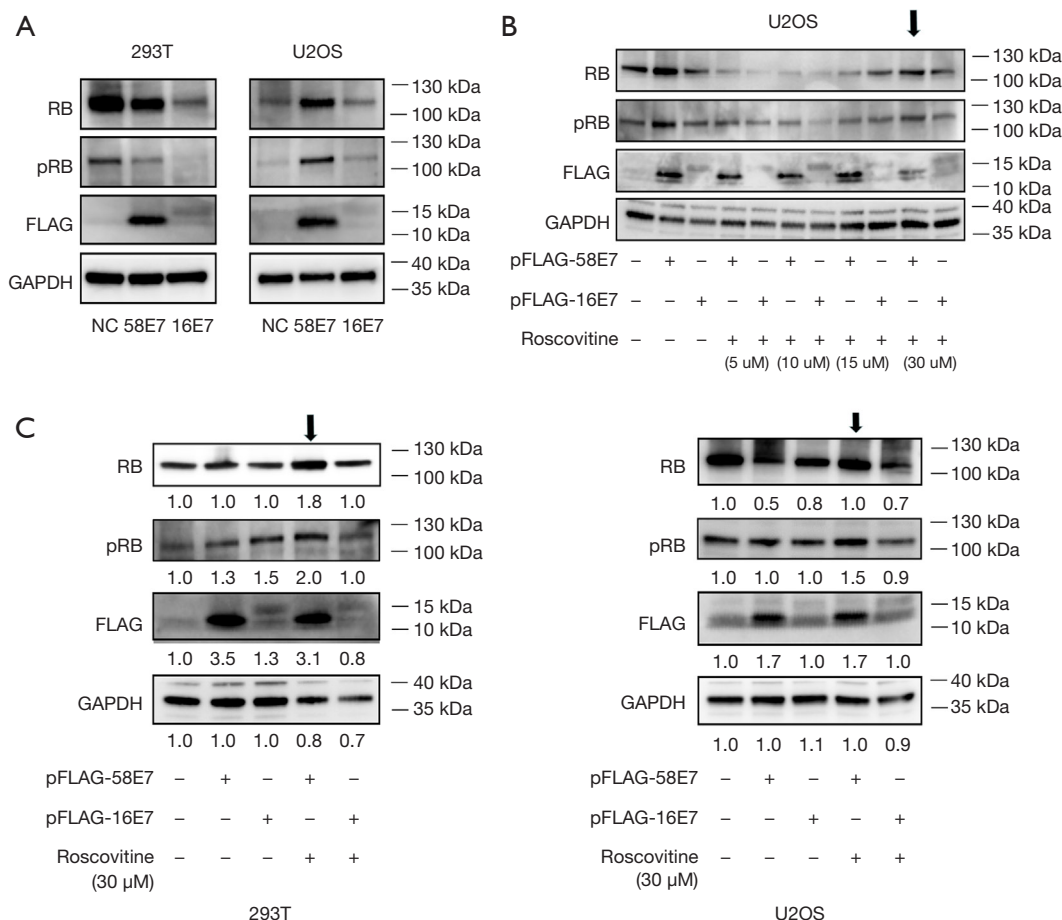


Figure 3 Cells with HPV16 E7 overexpression demonstrated greater Rb loss of function while those with HPV58 E7 overexpression demonstrated greater Rb phosphorylation. (A) At 48 h after the transfection of the HPV16 and HPV58 E7 plasmids into 293T and U2OS cells, the protein level of pRb and Rb was analyzed via Western blotting. (B) At 48 h after transfection of HPV16 and HPV58 E7 plasmids into U2OS cells treated with roscovitine (5 μM, 10 μM, 15 μM, 30 μM), the expression of pRb and Rb was analyzed via Western blotting. (C) At 48 h after transfection of HPV16 and HPV58 E7 plasmids into 293T and U2OS cells treated with roscovitine (30 μM), the expression of pRb and Rb was analyzed via Western blotting. GAPDH was used to quantify the relative levels of pRb and Rb expression. HPV, human papillomavirus; NC, negative control.

and conduct assays in different time points to identify the different functions between HPV16 E7 and HPV58 E7. The difference of HPV E7 function on Rb may account for their difference in carcinogenic ability, and thus blocking the E7-Rb pathway may be the key to stopping the progression of cervical lesions.

Roscovitine, a CDK2 inhibitor capable of inhibiting Rb hyperphosphorylation, may be a candidate for restoring Rb function and thus reversing the effect of HPV E7. Thus, we used roscovitine (30 μM) to treat 293T and U2OS cells and found that Rb impaired by E7 overexpression was restored,

especially in the HPV58 E7 overexpression group. A similar situation was observed in the zebrafish model. Our results further confirmed the *in vitro* findings and suggest that the inhibition of Rb phosphorylation may be a viable approach to counteracting the role of HPV E7 in inducing the development and progression of cervical cancer, with roscovitine being the most promising drug in this regard.

Conclusions

HPV16 possesses a stronger carcinogenic ability than

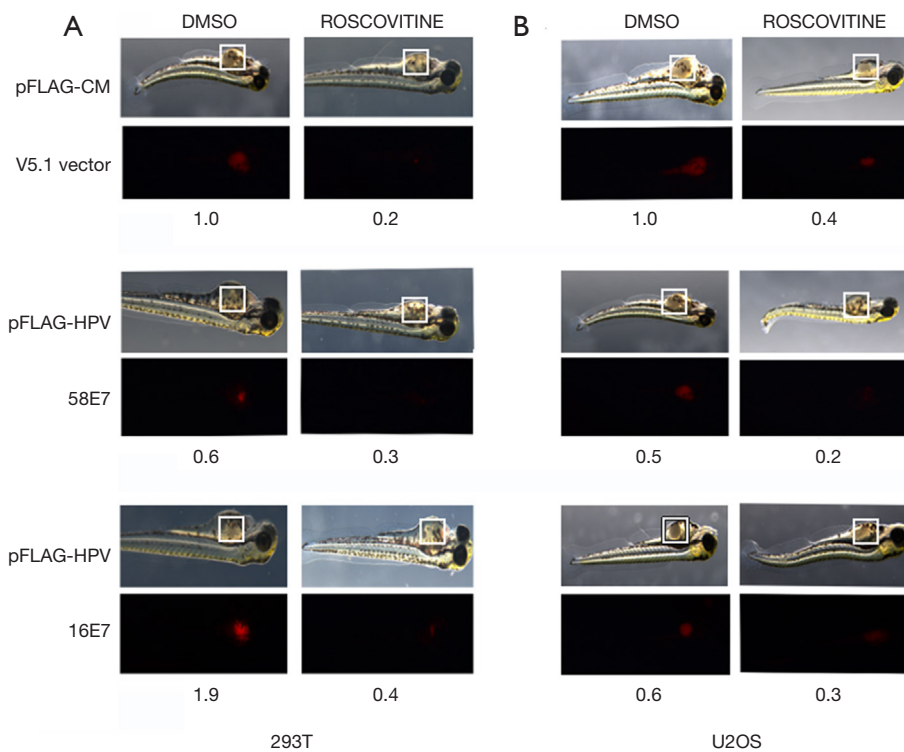


Figure 4 Roscovitine restored Rb expression in 293T and U2OS cells and decreased cell activity in the zebrafish model. The activity of 293T (A) and U2OS cells (B) was observed after transfection with HPV16 and HPV58 E7 plasmids and treatment with roscovitine (30 μ M). DMSO, dimethyl sulfoxide; HPV, human papillomavirus.

does HPV 58, and roscovitine may be a candidate drug for restoring Rb function and blocking HPV-induced carcinogenesis.

Acknowledgments

A portion of this study has been accepted for an oral presentation at the International Gynecologic Cancer Conference (https://ijgc.bmj.com/content/29/Suppl_3/A17.2). The zebrafish were kindly provided by Prof. Xu Pengfei, at Zhejiang University. The zebrafish used in our experiment were maintained in the Zhejiang University zebrafish facility.

Funding: The research was supported by National Natural Science Foundation of China (No. 82103200) and the Zhejiang Natural Science Foundation (No. LQ22H160033).

Footnote

Reporting Checklist: The authors have completed the

ARRIVE reporting checklist. Available at <https://tcr.amegroups.com/article/view/10.21037/tcr-23-1211/rc>

Data Sharing Statement: Available at <https://tcr.amegroups.com/article/view/10.21037/tcr-23-1211/dss>

Peer Review File: Available at <https://tcr.amegroups.com/article/view/10.21037/tcr-23-1211/prf>

Conflicts of Interest: All authors have completed the ICMJE uniform disclosure form (available at <https://tcr.amegroups.com/article/view/10.21037/tcr-23-1211/coif>). The authors have no conflicts of interest to declare.

Ethical Statement: The authors are accountable for all aspects of the work in ensuring that questions related to the accuracy or integrity of any part of the work are appropriately investigated and resolved. This study was conducted in accordance with the Declaration of Helsinki (as revised in 2013) and was approved by the

institutional review board of the Women's Hospital of Zhejiang University (approval No. IRB-20230341-R). The requirement for individual consent was waived due to the retrospective nature of the analysis. All animal experiments were performed under a project license (No. ZJU20230472) granted by committee ethics board of Zhejiang University and in compliance with the institutional guidelines for the care and use of animals.

Open Access Statement: This is an Open Access article distributed in accordance with the Creative Commons Attribution-NonCommercial-NoDerivs 4.0 International License (CC BY-NC-ND 4.0), which permits the non-commercial replication and distribution of the article with the strict proviso that no changes or edits are made and the original work is properly cited (including links to both the formal publication through the relevant DOI and the license). See: <https://creativecommons.org/licenses/by-nc-nd/4.0/>.

References

- Singh D, Vignat J, Lorenzoni V, et al. Global estimates of incidence and mortality of cervical cancer in 2020: a baseline analysis of the WHO Global Cervical Cancer Elimination Initiative. *Lancet Glob Health* 2023;11:e197-e206.
- zur Hausen H. The role of papillomaviruses in anogenital cancer. *Scand J Infect Dis Suppl* 1990;69:107-11.
- Smith JS, Lindsay L, Hoots B, et al. Human papillomavirus type distribution in invasive cervical cancer and high-grade cervical lesions: a meta-analysis update. *Int J Cancer* 2007;121:621-32.
- Sung H, Ferlay J, Siegel RL, et al. Global Cancer Statistics 2020: GLOBOCAN Estimates of Incidence and Mortality Worldwide for 36 Cancers in 185 Countries. *CA Cancer J Clin* 2021;71:209-49.
- Li K, Li Q, Song L, et al. The distribution and prevalence of human papillomavirus in women in mainland China. *Cancer* 2019;125:1030-7.
- Zhu X, Wang Y, Lv Z, et al. Prevalence and genotype distribution of high-risk HPV infection among women in Beijing, China. *J Med Virol* 2021;93:5103-9.
- Li X, Xiang F, Dai J, et al. Prevalence of cervicovaginal human papillomavirus infection and genotype distribution in Shanghai, China. *Virology* 2022;19:146.
- Xu HH, Wang K, Feng XJ, et al. Prevalence of human papillomavirus genotypes and relative risk of cervical cancer in China: a systematic review and meta-analysis. *Oncotarget* 2018;9:15386-97.
- Moody CA, Laimins LA. Human papillomavirus oncoproteins: pathways to transformation. *Nat Rev Cancer* 2010;10:550-60.
- Scarth JA, Patterson MR, Morgan EL, Macdonald A. The human papillomavirus oncoproteins: a review of the host pathways targeted on the road to transformation. *J Gen Virol* 2021;102:001540.
- Martinez-Zapien D, Ruiz FX, Poirson J, et al. Structure of the E6/E6AP/p53 complex required for HPV-mediated degradation of p53. *Nature* 2016;529:541-5.
- Aarthy M, Kumar D, Giri R, et al. E7 oncoprotein of human papillomavirus: Structural dynamics and inhibitor screening study. *Gene* 2018;658:159-177.
- Narasimha AM, Kaulich M, Shapiro GS, et al. Cyclin D activates the Rb tumor suppressor by monophosphorylation. *Elife* 2014;3:e02872.
- Ma X, Yang M. The correlation between high-risk HPV infection and precancerous lesions and cervical cancer. *Am J Transl Res* 2021;13:10830-6.
- Sigurdsson K, Taddeo FJ, Benediktsdottir KR, et al. HPV genotypes in CIN 2-3 lesions and cervical cancer: a population-based study. *Int J Cancer* 2007;121:2682-7.
- Tatar B. Incorporating HPV 33 and cytology into HPV 16/18 screening may be feasible. A cross-sectional study. *Arch Gynecol Obstet* 2023;308:183-91.
- Wang X, Zeng Y, Huang X, et al. Prevalence and Genotype Distribution of Human Papillomavirus in Invasive Cervical Cancer, Cervical Intraepithelial Neoplasia, and Asymptomatic Women in Southeast China. *Biomed Res Int* 2018;2018:2897937.
- Wang Z, Li Z, Li J, et al. Prevalence and Distribution of HPV Genotypes in 1387 Women with Cervical Intraepithelial Neoplasia 2/3 in Shanxi Province, China. *J Cancer* 2018;9:2802-6.
- Khattak F, Haseeb M, Fazal S, et al. Mathematical Modeling of E6-p53 interactions in Cervical Cancer. *Asian Pac J Cancer Prev* 2017;18:1057-61.
- Bhat D. The 'Why and How' of Cervical Cancers and Genital HPV Infection. *Cytojournal*. 2022;19:22.
- Olmedo-Nieva L, Muñoz-Bello JO, Contreras-Paredes A, Lizano M. The Role of E6 Spliced Isoforms (E6*) in Human Papillomavirus-Induced Carcinogenesis. *Viruses* 2018;10:45.
- Antonio-Véjar V, Ortiz-Sánchez E, Rosendo-Chalma P, et al. New insights into the interactions of HPV-

16 E6*I and E6*II with p53 isoforms and induction of apoptosis in cancer-derived cell lines. *Pathol Res Pract* 2022;234:153890.

23. Sofiani VH, Veisi P, Rukerd M, et al. The complexity of human papilloma virus in cancers: a narrative review. *Infect Agent Cancer* 2023;18:13.

Cite this article as: Zou J, Li Y, Chen T, Zhu C. An E7-retinoblastoma protein pathway mechanism may account for the higher carcinogenic ability of HPV16 over HPV58 in cervical cancer. *Transl Cancer Res* 2024;13(4):1876-1886. doi: 10.21037/tcr-23-1211

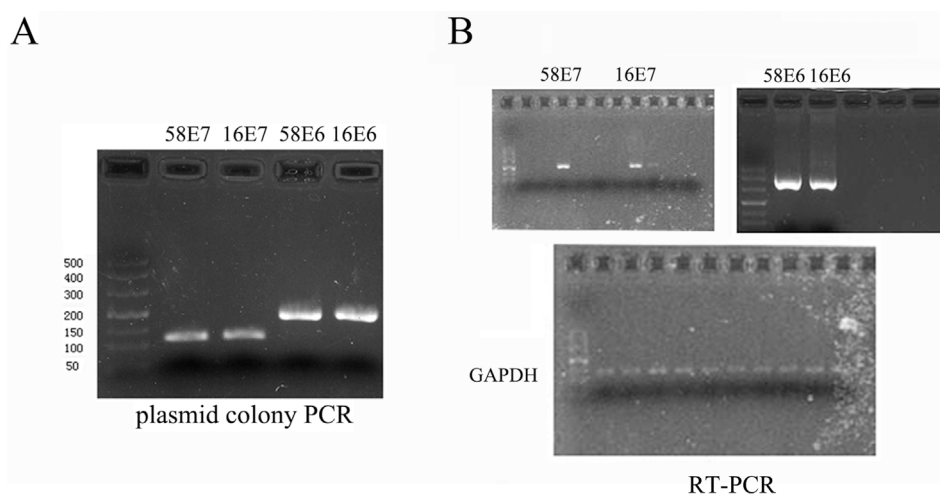


Figure S1 The plasmid colony PCR of Pflag-CMV5.1-HPV16/58 E6 and E7 and their expression according to RT-PCR. (A) The colony PCR of plasmids containing the HPV16/58 E6 and E7 genes. (B) The expression of HPV16/58 E6 and E7 according to RT-PCR. RT-PCR, reverse transcription-polymerase chain reaction.